Silicon (2018) 10:471–482
DOI 10.1007/s12633-016-9477-x

ORIGINAL PAPER

Influence of Industrial Solid Waste on the Chemical and Mechanical Properties of Traditional Glaze-Ceramics

T. D. Abd-Elaziz[1] · **F. M. Ezz-Eldin**[2]

Received: 21 June 2015 / Accepted: 29 August 2016 / Published online: 5 January 2017

Abstract New glaze compositions were synthesized from combinations of ceramic glaze and cement kiln dust. The products show very good chemical resistance to acid and alkaline corrosion, with no visual changes on the surfaces of the samples. This resistance can be attributed to the very well balanced composition of wastes and commercial ceramic glaze materials. Corrosion data reveal the results of mass loss either at 25 °C or 100 °C. The mass loss is very low, showing that it is possible to develop glazes with excellent chemical resistance to strong acid and alkaline solutions corrosion starting from different concentrations of cement kiln dust associated with commercial ceramic glaze materials. The IR spectra of the prepared samples show characteristic bands related to the vibrations of triangular and tetrahedral borate and tetrahedral silicate groups together with metal-oxide groups. The surface hardness data of the glazes determined by Mohs are found to be 5–6 at early immersion times up to ∼9 days, but there is obvious deterioration beyond 9 days. The results point out that it possible to deepen the understanding of the mechanisms of elements released through the chemical attack and their implications on microstructural and mechanical degradation of the working surface of glazed ceramic tiles.

Keywords Glazes · CKD waste · Corrosion · Surface analysis · FTIR · Hardness

✉ T. D. Abd-Elaziz
tamegc@hotmail.com

[1] October University for Modern Sciences and Arts (MSA), 6th October City, Egypt

[2] National Center for Radiation Research and Technology, Atomic Energy Authority, Cairo, Egypt

1 Introduction

The re-use of materials gained from solid wastes reduces degradation of the living environment, which is the initial objective of solid-waste management. Several studies have revealed the possibility of using a wide variety of wastes to produce different types of ceramic-like materials as glasses and glass–ceramics [1–4]. In this context, the minimization of huge wastes produced by the cement industry is of great concern in most countries. For a sustainable future, it would be imperative to recycle as much of these wastes as possible, on one hand to alleviate the problem of environmental inconvenience caused by landfills and on the other hand to create a supply of inert materials that would meet the environmental laws and industrial policies [5].

Ceramics have come up as a trend to reduce the risks to humanity and the environment as well as offering the possibility of combining the special properties of conventional sintered glaze-ceramics with the distinctive characteristics of cement-kiln-dust (CKD) waste. Developing ceramic-glazes demonstrates the advantage of combining various remarkable properties in one material.

One of the characteristic properties of the material is its ability to resist the corrosive action of water, aqueous solution of acids, alkalis and salts etc. This resistance is known as chemical durability which depends on the structure, composition of the material, laboratory conditions, and the environment [6]. In the glass ceramic materials, the chemical durability is a function of many factors such as the ratios of the constituting oxides added and consequently the nature and the concentration of the crystalline phases formed, composition of the present residual glassy phase, all of which are controlled by the glass composition and applied heat treatments [7]. Microstructure can also be taken into consideration. The non-porous microstructure of the

Table 1 Composition of CKD and Portland cement (weight %)

Constituents	SiO_2	Al_2O_3	Fe_2O_3	MgO	K_2O	Na_2O	CaO	SO_3	Cl	I.L.
CKD	11.45	3.22	1.88	0.53	3.73	2.72	45.14	5.14	2.59	23.60
Portland Cement	20.36	5.33	3.97	2.1	0.14	0.48	63.77	2.72	0.03	19.10

glass-ceramics makes it possible to count on better chemical stability as compared with porous ceramics, which have a more extensive surface and greater penetrability to liquids and vapors [8]. The chemical stability of glass-ceramics determines their applications in different environments and is therefore of considerable practical importance. The mechanisms of reactions occurring between glass-ceramics and aqueous solutions, as well as the factors affecting the chemical durability, were studied. It is generally agreed that the chemical behavior of glass-ceramics is related to their crystalline phases formed and the residual glassy matrix [9]. The effect of acidic solutions on the different types of mineral phases has been studied by many authors [8, 10]. With respect to the acid mineral stability, some minerals are very resistant to the action of acids (nearly insoluble), however some authors have stated that high silica content has a tendency to improve glass-network interconnectivity and enhance chemical resistance by increasing the ratio of bridging oxygens [11].

This paper presents results regarding the corrosion behavior of the prepared cement dust glaze (CDG) soaked in high concentrated HCl, H_2SO_4 and NaOH solutions. In this work, chemical durability and hardness properties of glazes doped CKD derivatives have been studied with the focus on the principal role of CKD in modifying the chemical durability of the commercial glaze and topography of the surface. Finally, this study aims to know how the addition of CKD to the industrial glaze composition enables the CDG to resist high concentration acidic or alkaline solutions.

2 Experimental Procedure

2.1 Preparation of Glaze

The composition of cement dust compared to that of Portland cement is shown in Table 1. Also the composition of the industrial glaze frit is shown in Table 2. Compositions of the studied glaze were prepared as presented in Table 3. The addition of cement dust was with an augmentable amount in the investigated batches from 10 % to 50 % The melting of the weighed batches was carried out in alumina crucibles at 1400 ^oC up to 5 hr. The melts were rotated several times and the homogenized melts were poured in slightly warmed stainless steel molds of the required lengths (1 x 1 x 5 mm). The prepared samples were immediately transferred to an annealing furnace regulated at 500 ^oC. The muffle was switched off and left to cool over night at a rate of 20 ^oC/h.

2.2 X-ray Diffraction (XRD) Measurements

The X-ray diffraction (XRD) patterns of the prepared samples were recorded with a Philips X-ray diffractometer PW/1710; with Ni filter, and with monochromatised CuK_α radiation of wavelength 1.5418 Å at 40 KV and 30 mA. The peak profile recorded with good resolution, 1/8 deg/min., was performed and the approximate crystallite sizes at FWHM were determined from the X-ray diffraction data using the Scherrer formula; ($G = \lambda/D \cos\theta$) where G is the crystallite size, λ is the wavelength of the X-rays (1.5418), D is the width of the peak at half maximum and θ is the angle of incidence of the X-ray beam.

2.3 Chemical Durability

In order to establish the critical parameters for the experimental tests, the glaze thickness of all the products was determined on the polished cross section of the samples. The test of the chemical durability was carried out by the weight loss technique. The acidic attack was performed by exposing the glazed surface of the tiles to a different concentration of HCl solutions (0.5, 1.5, 4.5 M), at a constant temperature (˜25 ^oC). In addition, the same glaze samples were placed in a polyethylene beaker containing 40 cm^3 of other different leaching solutions (1.5 M H_2SO_4 or 1.5 M NaOH). The immersion time was varied from 1 up to 25 days at a constant temperature (˜25 ^oC) for all different leaching solutions; however, at 100 °C±2 °C (in HCl solutions) the examination duration is ranged from 2 up to 30 hours. After particular immersion times in each acid or base

Table 2 Composition of the industrial glaze frit (weight%)

B_2O_3	ZnO	$CaCO_3$	Na_2CO_3	Borax	Albite	Dolomite	Zircon	Sand
27.71	0.78	8.992	2.722	11.418	12.026	3.634	13.929	18.788

Table 3 Compositions of Cement-Dust-Glaze (CDG) (weight%)

Glaze no.	CKD	Frit	B_2O_3
C1	0	90	10
C2	10	80	10
C3	30	60	10
C4	50	40	10

solution each sample was carefully weighed three times before and after being immersed in the different solutions and the weight loss% was calculated. The correlation between the surface area (S) of the investigated samples and the volume (V) of the immersion solutions was kept constant as S/V= ˜0.053 cm^2/ml.

2.4 pH Measurements

The pH values for the leachate solutions were determined instantly, this test was performed using an Orion Research (601A) at 25 °C, with accuracy measurements ±0.01pH unit.

2.5 SEM and EDX Measurements

The surface morphology of the as-received and the leached tiles was observed by using a scanning electron microscope (SEM, Zeiss EVO 40, D) equipped with an energy-dispersive X-ray analyzer (EDS, Inca, Oxford Instruments, UK). The same system was used also to determine the quantitative chemical composition of the glazes and of selected areas, corresponding to the amorphous phases. The chemical compositions values, reported in Tables 4 and 5, are the average of almost five analyses performed in different areas and corrected with inner standards.

2.6 FTIR Measurements

Fourier transform infrared absorption spectra of the glazes were obtained with a recording FTIR spectrometer (type Mattson, 5000, USA). Powdered C3 glaze samples (2mg) were mixed with KBr powder (200 mg) and pressed with 5 tons/cm^2 to form thin transparent homogenous disks. Infrared absorption spectra within the range 400-4000 cm^{-1} were recorded immediately after the preparation of the disks. The IR measurements were carried out for the glaze samples before and after soaking in different concentrations of HCl leaching solutions (0.5, 1.5 and 4.5 mol/L).

2.7 Density and Absolute Hardness Measurements

The density of the samples was measured by considering the weights and dimensions of specimens, and bulk density by the Archimedes method using xylene as the immersion liquid. The estimated error is ±0.001 gm/cm^3. Absolute hardness tests were first performed on virgin developed glaze samples to compare them with the corroded glazes investigated in this work. The absolute hardness values were determined after following the Mohs scale of minerals. Mohs hardness scale scratch is based on ten minerals that are all likely available except diamond. The pristine and corroded developed glaze pieces (1 x 1 x 0.2 cm) were sparkled preceding the hardness measurement, and then scratched by utilizing the mineral found in the Mohs Scratch Test kit.

Table 4 EDX microanalysis performed on the virgin studied glazes (C1-C4) (weight%)

Element	C1	C2	C3	C4
Si	76.4	56.3	53.5	40.9
Ca	8.7	25.4	22.3	24.6
Mg	0.2	1.3	0.9	0.9
Na	0.6	1.1	1.8	0.8
K	2.5	2.0	2.1	1.6
Al	3.2	7.6	6.4	8.1
Fe	0.1	0.60	0.5	1.4
Zn	5.3	3.66	2.6	2.3
Zr	1.4	1.5	0.2	0.2

3 Results and Discussion

Due to the rapid increase in the quantities of solid wastes, affecting public health and the environment, efficient and sustainable solid waste-management must be considered as the most pressing issue on the agenda of developing countries and governments worldwide.

3.1 XRD Measurements

As seen in Fig. 1, the XRD patterns of the studied glaze samples are almost identical. The main part of the XRD patterns

Table 5 EDX microanalysis performed on the glazes (C1-C4) after being immersed in 1.5 M HC1 for 25 days at R.T. (weight%)

Element	Cl	C2	C3	C4
Si	63.2	52.3	51.7	37.7
Ca	16.1	22.4	27.8	41.8
Mg	1.9	1.8	2.5	1.0
Na	2.5	2.9	3.0	1.3
K	2.2	1.7	1.3	1.5
Al	7.4	9.3	8.6	8.9
Fe	0.1	0.6	0.6	1.9
Zn	7.1	9.0	13.6	6.7
Zr	1.2	0.7	0.8	0.2

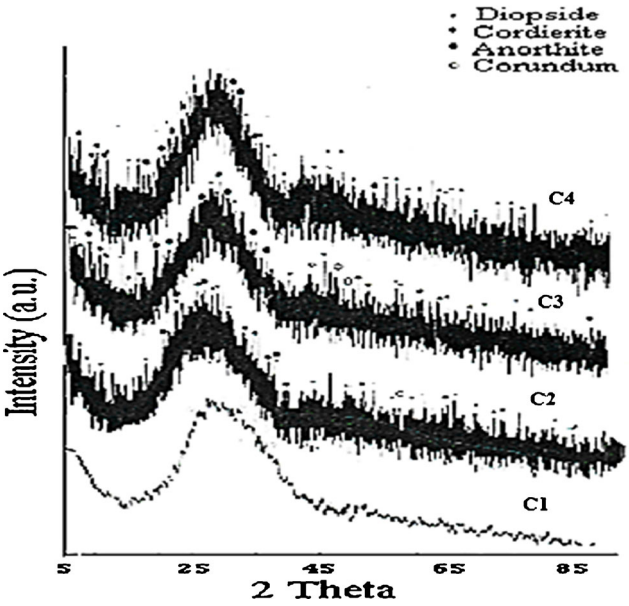

Fig. 1 The XRD patterns of the virgin studied glazes

confirms the amorphous character of the investigated samples. However, a few diffraction lines are also visible. The most relatively intensive peaks presented in the XRD patterns at around $2\theta = 5–85^{o}$ indicate the presence of micro and sub-micro phases which increase when CKD% was increased. As expected, addition of CKD to the glaze frit should have formed crystalline phases due to the presence of CaO and Fe_2O_3 (Table 1), although, due to the presence of a relatively noticeable percent of ZnO (˜0.8 %) in the frit (Table 2) it would inhibit the formation of crystalline phases and allow the formation of micro and sub-micro phases. The XRD patterns of all the tested glaze-ceramic samples are shown in Fig. 1. From these patterns the crystal phases such as $CaMgSi_2O_6$ (Diopside), $Mg_2Al_4Si_5O_{18}$ (Cordierite), $CaAl_2Si_2O_8$ (Anorthite) and Al_2O_3 (Corundum) were identified with the help of JCPD data [12]. The comparison of the XRD spectra, collected on the glaze powder of all the tested samples, shows that the amount of glassy phase progressively increases from sample C1 to sample C4. In particular, as regards C1 and C2, the glaze presents a rather low amount of glassy phase and zircon is the main crystalline phase with a small amount of quartz. Also, Fig. 1 shows an increase in the peak intensity of diopside, which suggests the growth of this crystal with columnar structure inside the glass phase, forming a glass–ceramic glaze [13, 14]. The peak intensity is smaller (at $2\theta = 40–50^{o}$); it can be interpreted by the fact that our samples hold a higher percentage of Fe_2O_3 (3.97 wt.%) present in CKD [15] and the intensity ratio between the strongest peak and other peaks becomes larger, which demonstrates that the crystalline grains grow with a highly preferred orientation when increasing CKD% [16].

3.2 Chemical Durability

3.2.1 At Room Temperature

Chemical durability of glazes was previously mostly studied as corrosion of the glassy phase. The glassy phase was attacked in strongly acidic and alkaline solutions similarly to conventional glasses.

Chemical durability of the different phases after immersion in the aqueous solutions was estimated both visually and based on the SEM images. In the most acidic solutions, ion exchange reaction of the alkalis and alkaline earths to hydrogen ions is assumed to occur followed by a formation of a silica rich layer and a partial peeling off of the layer [17, 18]. The surface of the fast-fired glaze shows columnar diopside crystals and a partly cracked and peeled-off silica rich layer [18].

It was reported that, in alkaline environments, the network structure of glass is continuously attacked and destroyed by hydroxyl attack [19–23]. Glaze-ceramic materials are considered as polycrystalline silicate solids containing a glassy phase and possess a valuable combination of the favorable properties of both glasses and ceramics [17]. The influence of different oxides on the durability of glasses and glassy glazes is well understood [17]. However, chemical resistance of glazes consisting of one or several crystalline phases embedded in a glassy matrix has not been fully and widely studied. Wollastonite and anorthite crystals devitrified from a fritted glaze have been reported to be attacked by acidic solutions [24]. Wollastonite crystals in fast-fired raw glazes are attacked by acidic and also slightly with alkaline water solutions [25, 26]. The formation of crystalline phases in traditionally fired glazes takes place according to the equilibrium reactions and is controlled by the total oxide composition of the glaze. However, in a modern fast-firing process of floor tiles, the short firing cycle of 60-90 min restricts the extent of raw materials [27, 28]. The leaching results (Figs. 2 and 3) can be explained according to the postulations given in previous studies [17] which have shown that when sodium borosilicate glasses dissolve in acidic solutions, sodium and boron are selectively removed to produce hydrosilicate leached layers. In all cases, the structure of the leached glass is substantially different from that of the parent glass. It can be assumed that [20] some of the nonbridging oxygen (NBO) sites are converted into silanol (SiOH) groups via the $H^+ \leftrightarrow Na^+$ ion exchange:

$$\equiv Si - O^{-}Na^{+} + H_3O^{+} \rightarrow \equiv Si - OH + Na^{+} + H_2O \quad (1)$$

The large decrease in concentration of NBOs after ion exchange demonstrates that silanol groups in leached glass

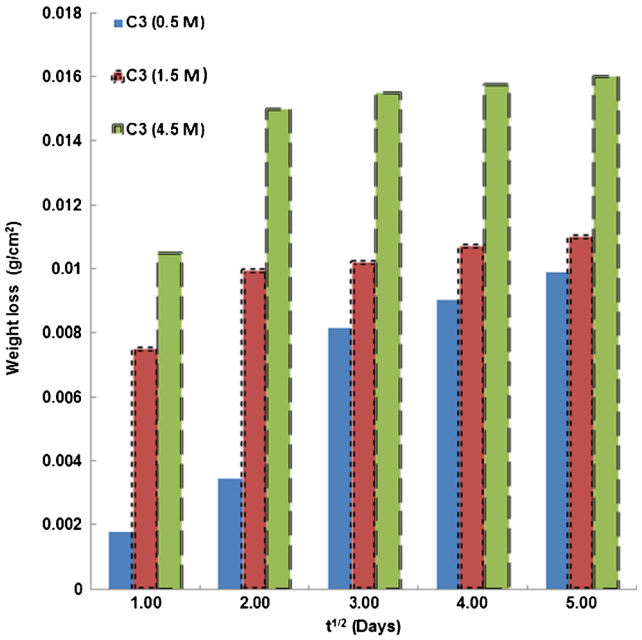

Fig. 2 The effect of different concentrations of the leaching solutions (0.5, 1.5 and 4.5 M HC1) on the corrosion (determined by weight loss (gm/cm^2)) of the studied glaze C3 after being immersed in the solutions up to 25 days

react with each other to form new Si-O-Si bonds via reaction such as:

$$\equiv Si - OH + HO - Si \equiv \rightarrow \equiv Si - O - Si + H_2O \qquad (2)$$

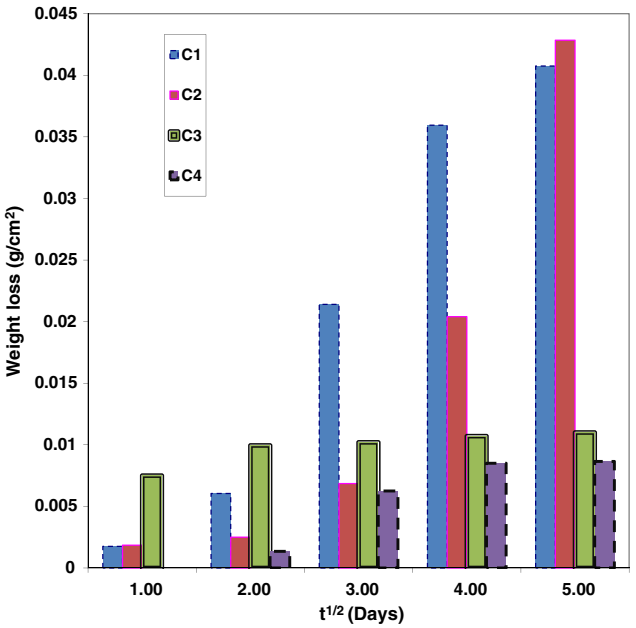

Fig. 3 The effect of the leaching solution (1.5 M HC1) on the corrosion (determined by weight loss (gm/cm^2)) of the studied glazes C1, C2, C3 and C4 after being immersed in the solution up to 25 days

If reaction (2) is to go to completion, the product would be amorphous silica and water. The fact that all the glazes have almost identical concentrations of both silanol groups and fourfold rings suggests that the structure of the hydrosilicate phases produced by leaching under acid conditions is independent of the structure of the parent glass. It appears that the initial network structure is broken down and reconstructed and eventually completely dissociated during leaching with high HCl concentration (4.5 mol/L). For borosilicate glasses, another important reaction leading to the formation of silanols is the hydrolysis of Si-O-B. It was suggested [29] that in acidic solutions hydrolysis of Si-O-B and B-O-B bonds (with either trigonal or tetrahedral borons) involves the electrophilic attack of protons on bridging oxygens (Reaction 3).

Reaction 3 explains why boron leaching is promoted in acidic solutions and why acidic solutions promote the conversion of fourfold boron sites to threefolds sites. Dissolution data suggest that the pH below which the bridging oxygen is protonated and subsequently hydrolyzed for both Si-O-B and B-O-B bonds is near 4 [29].

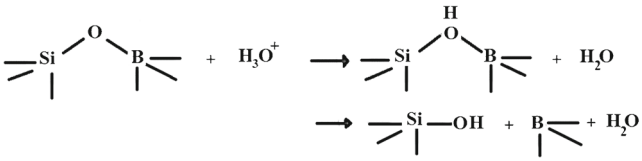

(3)

The network is transformed from a homogeneous diffusion barrier to a porous aggregate of colloidal silica particles in which diffusion is rapid and does not contribute to the generation of large tensile stress in leached layers, leading to crazing and spalling [30]. However, increasing immersion time up to 25 days leads to fast and high dissolution due to the detachment of the leached layer. The observed constancy or decrease in the weight loss when CKD% exceeds 30 % as observed in Fig. 3 can be interpreted by assuming that the increase of CKD introduces much CaO and other constituents which may reach constant solubility with HCl and saturation with less ability for further attack.

3.2.2 Effect of Different HCl Concentrations

The leaching results (Fig. 2) clearly demonstrate that the C3 glaze sample undergoes some structural changes during leaching in different concentrations of HCl aqueous solutions. Published results concerning the chemistry of silica indicate the formation of silanol groups during selective leaching which promotes the observed structural changes [31]. Silanol groups promote the hydrolysis of adjacent Si-O-Si bonds, leading to depolymerization and dissolution of the silicate network. Simultaneously silanol groups exhibit

a strong tendency to condense with each other, reforming Si-O-Si bonds and promoting repolymerisation of the network causing false stability in durability observed in the interval times (4-25 days) indicating that the repolymerisation of the silicate network increases relatively with increasing time of immersion. Also, increasing HCl concentrations, leads to increase of Cl^- anion to a sufficient level to act together with cations. In addition, raising the potency of the acidic range enhances the degree of dissolution of alkali elements in glazes and reduces hydrated layer dissolution. Thus, the effect of raising the concentrations of H^+ in solution enhances the ion exchange variation between H^+ protons, or H_3O^+ ions and alkali ions.

3.2.3 Effect of Temperature

The effect of temperature is of special interest with regard to accelerated tests of chemical durability. the kinetic reaction is not altered by the consequence of temperature but orders the rate controlling corrosion mechanism [32]. However, on raising temperature up to ~100 °C, total dissolution controls the leaching rate, whereas at room temperature (~25 °C) selective leaching controls the rate. The solubility of silica in solution is quite low at ~25 °C; hence at this temperature silica is relatively insoluble and thereby forms a layer of hydrated silica on the surface. As R_2O and RO are leached into solution, the silica layer thickens. At 100 °C, the hydrated silica can enter the solution as silicic acid. Likewise, R_2O and RO are continuously leached into solution. The relative rate at which these two processes occur determines the extent of leaching observed in Fig. 4.

3.2.4 Effect of Different Immersion Solutions

Figure 5 shows the corrosion behavior of the glaze (C3) after been soaked in 1.5 M (HC1, H_2SO_4 or NaOH) solutions for 25 days at R.T. Only minor changes were observed in the glaze durability when the glaze (C3) was immersed in NaOH solution, but, there is an obvious deterioration when the glaze specimen was soaked in H_2SO_4 solution.

Effect of H_2SO_4 There is similarity in the reaction of H_2SO_4 and HCl solutions (Fig. 5) on the corrosion trend for the investigated glazes that may be assumed to be due to the high dissociation (ionization) of these acids causing sufficient release of H^+ or H_3O^+ ions, and consequently preceding the attack / hydrolysis of the glaze. The progressive release of both anionic and cationic components from the glaze sample begins additional and total dissolution due to the solubility of liberated alkali ions.

Effect of NaOH Solution It is noticeable from the corrosion data (Fig. 5) that, the sodium hydroxide (1.5 mol/L) gives a lower corrosion effect in contrary to the recognized fact that sodium hydroxide solution severely corrodes ordinary soda-lime-silica glass since it attacks both the network

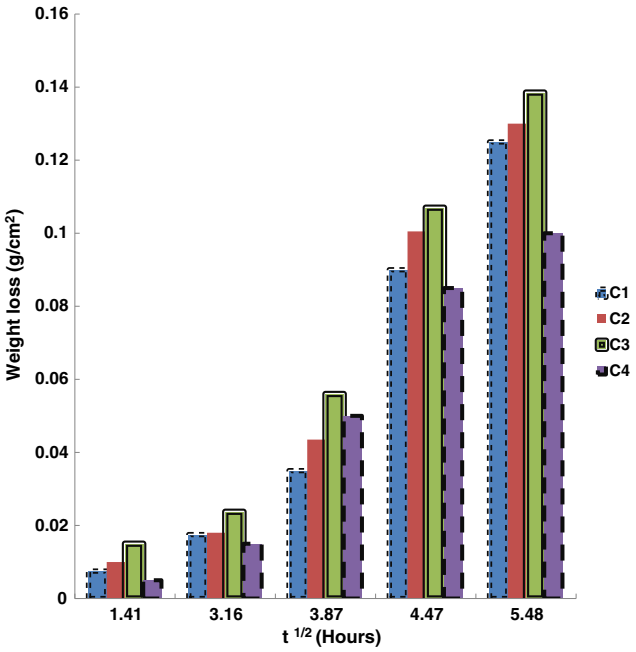

Fig. 4 The effect of the leaching solution (1.5 M HC1) on the corrosion (determined by weight loss (gm/cm^2)) of the studied glazes C1, C2, C3 and C4 after being immersed in the solution up to 30 hours at ~100°C

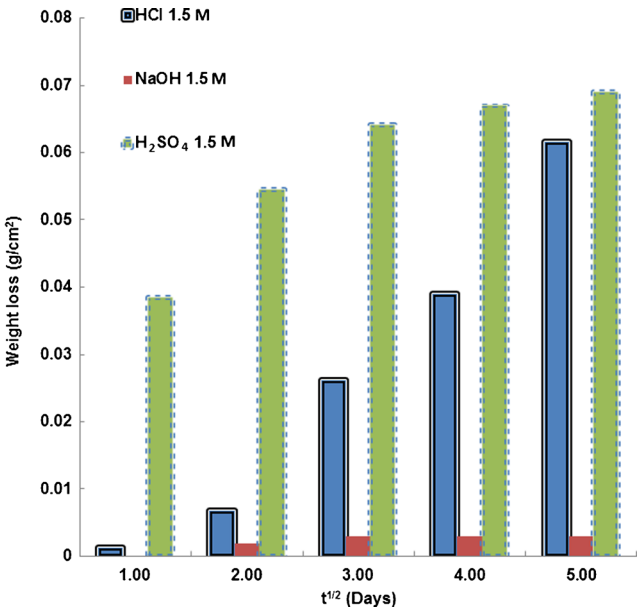

Fig. 5 The effect of different kinds of the leaching solutions 1.5 M (HC1, H_2SO_4 and NaOH) on the corrosion (determined by weight loss (gm/cm^2)) of the studied glaze C3 after being immersed in the solutions up to 25 days

modifiers and the silica network itself. Due to the high lime content in our glaze samples there are screening or controlling factors which delay the ion exchange reaction through the development of gelatinous $Ca(OH)_2$ layers. Clark et al. [33] studied this corrosion phenomenon and they accredited this anomalous behavior to the development of a Ca enriched zone ˜1500 Å thick within the Na depleted layer. Another explanation for this phenomenon was ascribed to either microphase separation and/or the action of lime in silicate glasses which may be unequally higher than in other glasses [34].

3.3 pH Measurement

The experimental data indicate that the variation in pH values is relatively dependant on both CKD% and the corrosion mechanisms (Fig. 6), i.e. by increasing either CKD% or weight loss % the pH values are increased. Our results can be interpreted by assuming that the increase of CKD introduces much CaO and other constituents which may reach constant solubility with HCl and saturation with less ability for further attack, Also, repolymerisation of the silicate network increases relatively with increasing time of immersion. At 100 °C Fig. 7 the pH increase is assumed to be mainly due to an ion exchange reaction of calcium in the crystals with hydrogen ions in the solution. Moreover, the observed increase in the pH values as the CKD% was raised is owing

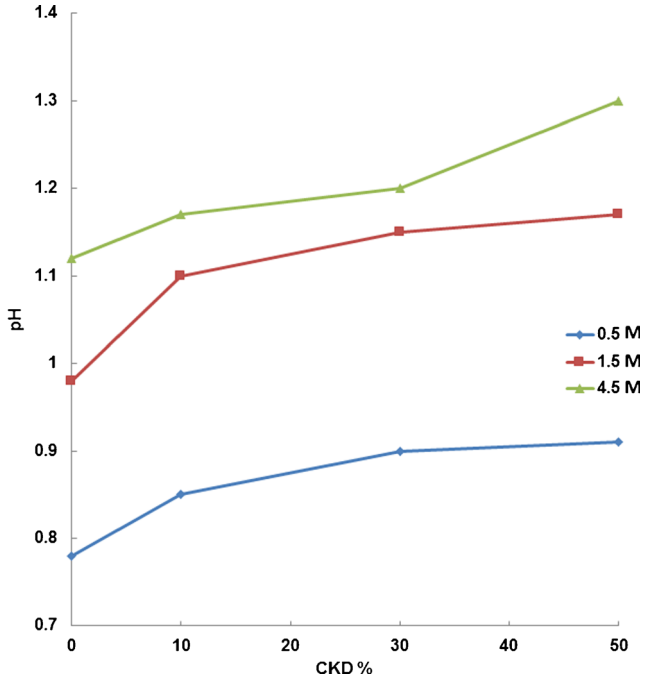

Fig. 6 The effect of increasing CKD% in glazes after being immersed in different HCl concentrations (0.5, 1.5 and 4.5 M) up to 25 days,on the pH values of the leaching solutions

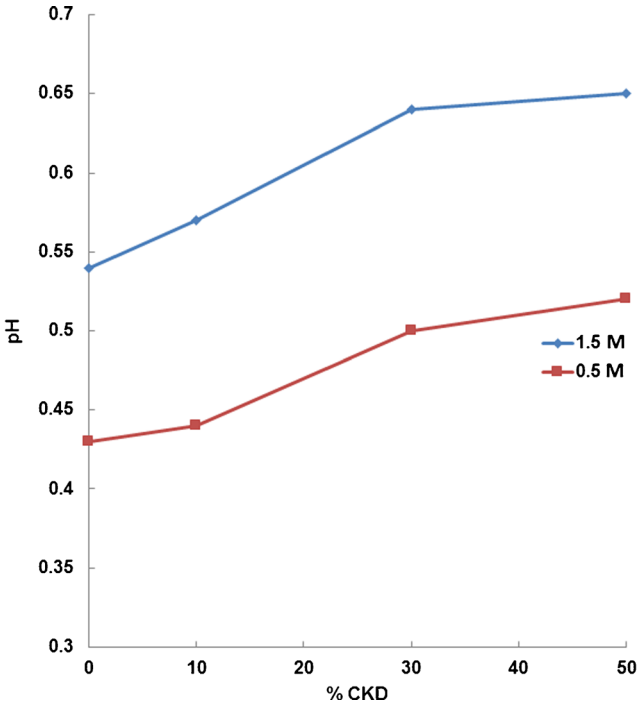

Fig. 7 The effect of increasing CKD% in glazes after being immersed in different HCl concentrations (0.5 and 1.5 M) up to 30 hours at 10^{0o}C,on the pH values of the leaching solutions

to the presence of K_2O and CaO which form KOH and $Ca(OH)_2$ by severe attack caused by this high temperature.

3.4 SEM and EDX Measurements

Micrographs of glaze surface (C3) before and after soaking in 0.5, 1.5 and 4.5 M HCl solutions for 25 days are shown in Fig. 8. The images are taken for the same surfaces and at identical locations of the surface line profile given in Fig. 8. From these images grey holes are observed in the surface structure. After soaking in 0.5 M HCl solution, these holes are assumed to be partly dissolved and residual crystals are assumed to be nucleated. The crystals are seen in the 1.5 M HCl surface as tiny peaks, and after soaking, holes can be observed instead. After soaking in 4.5 M HCl, clear changes in micro-roughness of the surface can be verified. The observed differences in softness degree can be attributed to the rise in micro-roughness achieved by selective dissolution from the glaze (C3) surface.

The microanalysis (EDX) of the surface of the studied glazes before and after being subjected to the corrosion test (Table 4) and (Table 5) respectively, confirmed a noticeable decrease in the K_2O and SiO_2 content and a relative increase of Na_2O, CaO, Al_2O_3, MgO and ZnO content due to their leaching and precipitation as, for instance, carbonate and silicate phases. It is well known that the effect of zinc

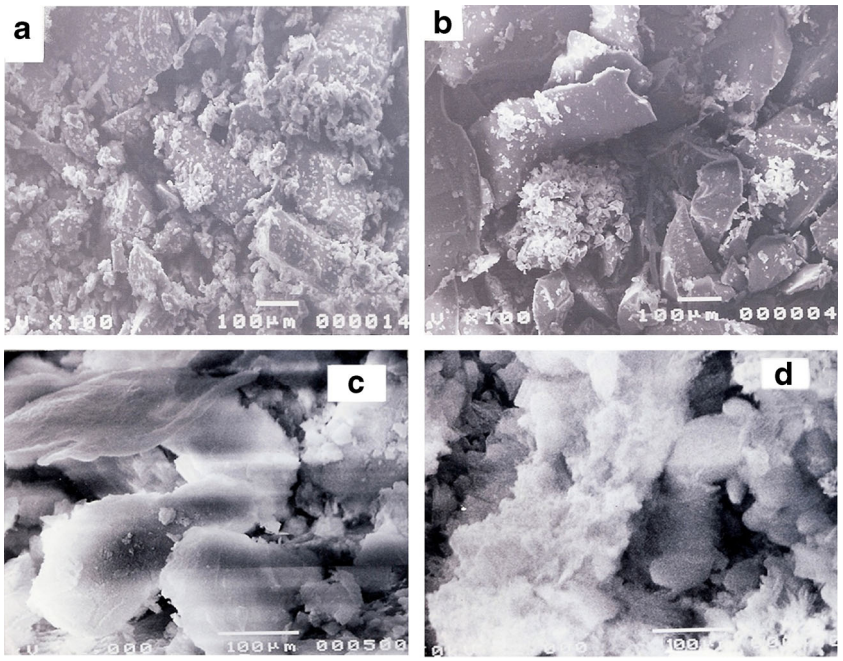

Fig. 8 SEM for the specimen C3 before and after being soaked in different HCl concentrations for 25 days; (**a**) Virgin sample (**b**) 0.5 M, (**c**) 1.5 M and (**d**) 4.5 M

on surface enrichment of elements such as insoluble silicate [27], is because alkali ions are preferably leached out. In our sample (C1), the ZnO% is relatively high (˜5.3) to allow the formation of a considerable quantity of a surface layer of zinc silicate on the glaze surface. This protective layer was also suggested by other authors [28]. Moreover, multiply charged ions such as Zn^{2+}, which are larger and less mobile than highly mobile alkali ions, can block the nonbridging oxygen sites. Then, the zinc ions might act as inhibitors or cause retardation of the diffusion process. This fact can be justified by considering that alkali cations break the Si-O-Si network through the introduction of nonbridging oxygen sites (e.g. Si-O-Na^{+}). These suggested reasons explain why there is a gradual decrease in silica and increase in zinc at the glaze surface for the studied glazes (C1→ C4) (Table 5). The K^{+} ions are found to be reduced on the surfaces, due to the high ion-exchange between K^{+} ions and H^{+} ions from the HCl solution. It is worth noting the increase or decrease in deposited elements at the glaze surface (Table 5) between the studied glazes (C1-C4) and the remarkable differences in their contents (Tables 1, 2 and 3) for the analogous elements (Ca, K, Si etc) and, to the variations in the replaced CKD % (0 %-50 %).

3.5 FTIR Measurements

Studies of the composition dependence of IR absorption spectra show that these glazes are built up of the Na_2O–CaO–B_2O_3–SiO_2–Al_2O_3–Fe_2O_3. SiO_2 is a well-known glass former and expected to participate in the glass network with tetrahedral $[SiO_{4/2}]^0$ units and all the four oxygens in SiO_4 tetrahedral are shared. On addition of modifiers like Na_2O, the Si–O–Si linkage is broken and the structure is de-polymerized with the formation of $[SiO_{3/2}O]^-$, $[SiO_{2/2}O_2]^{2-}$, $[SiO_{1/2}O_3]^{3-}$ groups [35]. The absorption band at∼465 cm^{-1} is characteristic of Si–O rocking motion [36, 37]. From the spectra the vibrational modes observed at about **1060** cm^{-1} are due to the stretching vibrations of $[BO_4]$ units [38]. The band centered at ≈**1096** cm^{-1}, was attributed to Si–O–Fe vibrations [39]. In addition, the IR spectra also exhibited a weak band at∼**725** cm^{-1} which is related to the stretching vibration of the Al–O bonds with $A1^{3+}$ in four-fold coordination [40]. This peak is shifted towards 800 cm^{-1} at the high HCl concentration (4.5 mol /L). Furthermore the experimental results (Fig. 9) prove the formation of the ∼**1645** cm^{-1} (H-O-H) and ∼**3100–3500** cm^{-1} bands in all glazes generally affiliated to the stretching and transferring modes for (OH) groups, H_2O and SiOH groups. It is well known that [41] the observed reduction in the bands intensity can be due to deterioration processes of the component of glaze C3 and it appears that the noticeably severe action of HCl solution, could be related to stimulated adsorption of H_2O currently present in the leachant solution. Superimposing on these curves for the silica matrix, glaze specimen (C3) corroded by different HCl concentration solutions reveals fairly sharp principal silicate bands and those due to OH, carbonate, hydrogen are slightly diminished [42, 43]. Another two bands can be easily seen, namely the characteristic absorptions of the calcium carbonate group ($CaCO_3$) at∼**1415** cm^{-1} and ∼**900** cm^{-1} [44]. Generally, the experimental IR data show the major structural assemblage of the corroded samples remains unchangeable as demonstrated by the preservation of the

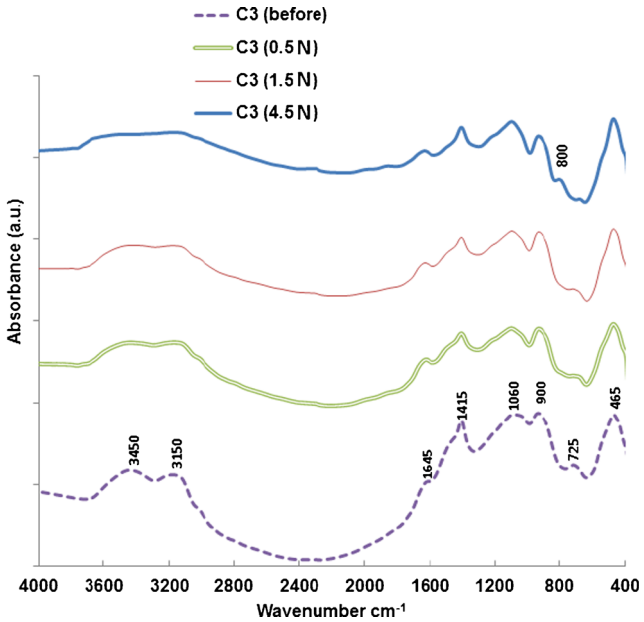

Fig. 9 The FTIR absorbance spectra for the specimen C3 before and after being soaked in different HCl concentrations (0.5, 1.5 and 4.5 M) for 25 days

principal characteristics of glaze samples. This designates the high durability of the silicate network following leaching to a great extent.

3.6 Density and Absolute Hardness

In general, the addition of species that enter the interstices of the vitreous network tends to increase the density by reducing the free volume, and addition of other ions to the glaze will alter the density in proportion to the mass of the added ions relative to that of the ions already present in the glaze [17]. Thus, the observed rise in glaze density shown in Table 6 may be correlated with the increase in the amount of cement dust waste introduced which contains a large amount of lime, where CaO decreases the number of nonbridging oxygens and reduces the free volume. It has been reported [29] that the glaze portion has a leached layer after basic (pH=12) dissolution but not after acidic (pH=0) dissolution.

An ion exchange reaction during the corrosion test may lead to the creation of M-OH and therefore cracking of a depleted layer [45]. On the other hand, the residual stress of the glaze created during the melting process and/or cooling may cause the cracking of a corroded layer throughout leaching. In addition, drying may cause further cracking of this layer analogous to the case of gel drying [46, 47].

It is well known that silicate glasses are generally brittle [48]. Their stress intensity factor (SIF) is very low, but the actual situation is even worse for glass in ambient conditions, as the tip of a surface crack undergoing a SIF of half the critical value, actually is slowly running. The crack speed does not depend on the environment; it increases sharply with SIF but levels off at some characteristic speed. As the strength of glass is controlled by the size of flaws, the fatigue effect is related to the growth of cracks (stress corrosion) during aging in the given environment under load. Also, the stress corrosion issue requires a careful control of the residual stress.

Our hardness results (Figs. 10 and 11) demonstrate that there is a decrease in the Mohs hardness values in the early periods of immersion times (up to ~10 days) followed by a stability in the absolute hardness values. This behavior is due to the progressive alkaline leaching out of the glass, and this change in the chemical composition at the tip of the crack is responsible for the fatigue limit rather than a geometrical change (blunting). The constancy of hardness values after long immersion times (10-25 days), can be attributed to the formation of silanol groups which can be associated with repolymerisation reactions

Table 6 Effect of CKD% on the density and absolute hardness for the virgin samples

Properties of virgin samples				
Samples	C1	C2	C3	C4
Density (g/cc)	2.42	2.5	2.55	2.91
Hardness (Mohs scale)	5.5:6	5.5:6	5.5:6	6:6.5

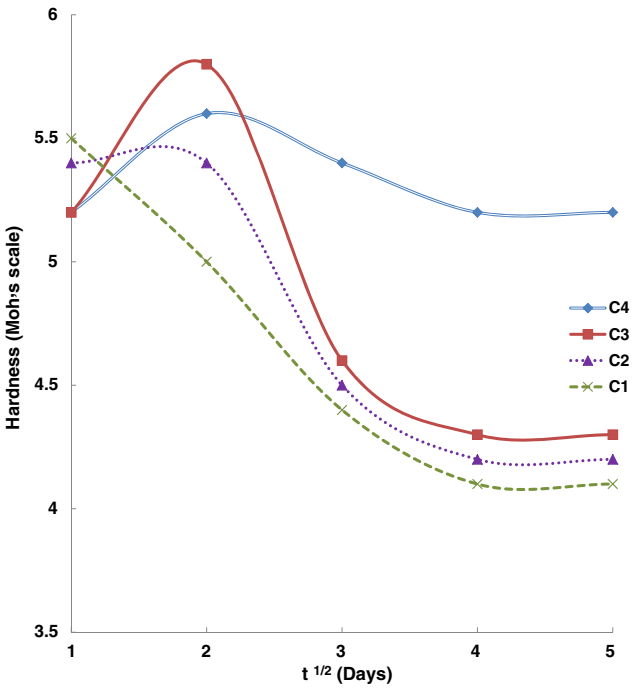

Fig. 10 The effect of the leaching solution (1.5 M HC1) on the absolute hardness values of the studied glazes C1, C2, C3 and C4 after being immersed in the solution up to 25 days

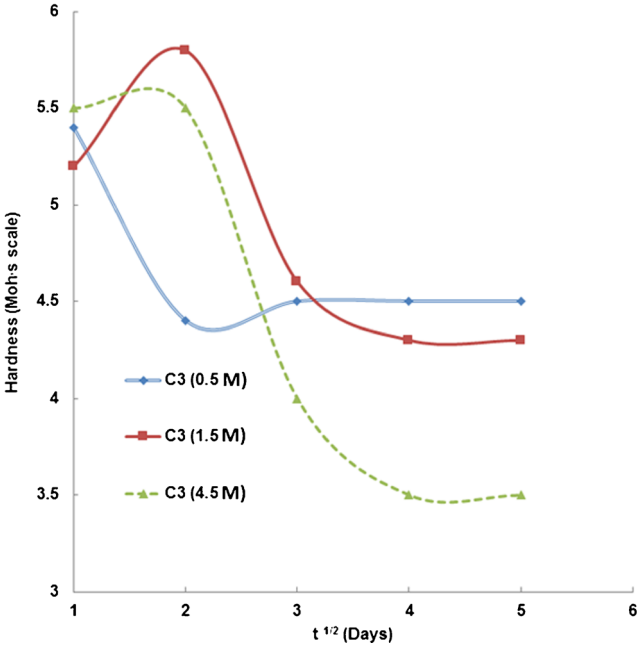

Fig. 11 The effect of different concentrations of the leaching solutions (0.5, 1.5 and 4.5 M HC1) on the absolute hardness values of the studied glaze C3 after being immersed in the solutions up to 25 days

involving the silicate network. It has been suggested that [20] the extent of network repolymerisation and the nature of the leached glass structure are controlled in large part by the concentration and distribution of silanol groups created in the glaze during leaching. Thus, it is possible to make predictions concerning how the glaze composition, structure, and solution chemistry should influence the repolymerisation process and leaching kinetics. In addition, the ease with which the network will repolymerize should increase as the number of silanols created during leaching increases. No polymerization should be observed for fused silica and glasses or glazes with high silica content which should be resistant to repolymerisation while alkali silicate with high alkali content should be very susceptible to repolymerisation. Moreover, alkali aluminosilicate or borosilicate should not undergo repolymerisation in the neutral pH regime, but should undergo repolymerisation below pH 4 where selective leaching of Al or B leads to the formation of silanols, and this is our case. Also, Fig. 10, shows successive increase in hardness after ˜10 days from C1 to C4 and this increase is relative to the amount of CKD added which is responsible for the hardness characteristic of the glaze due to its high content of CaO, MgO and Fe_2O_3. In addition, the compositions of the glazes in these samples have relatively high content of stronger zircon and dolomite.

The observed degradation in hardness (Fig. 11) at high HC1 concentrations can be accredited to the attack of solution on the entire surface mainly within the microcracks, being curved at both tips and subsequently diminishing the hardness. Furthermore, it should be stated in agreement with Ezz-Eldin et al. [49], and Ezz-Eldin [50], that the energy of the glass surface materials similarly can result in an earlier fracture formation. When a flaw is consequently corroded, its radius is enlarged at the crack end. This corresponds to a compaction of the crack and therefore has the effect of raising the strength. This can clarify the observation that glazes can be broken more easily after being scratched than they can after some elapsed time. As well, we can suppose that numerous stress relaxations may happen after the penetration of the sodium ions during the melting process.

4 Conclusion

In the present work, four series of new formulated glazes have been produced from combinations of industrial ceramic glaze and cement-kiln-dust waste in the range of interest which can be used to replace industrial ceramic glaze in a proportion of up to 50 % in weight. It can be concluded that CKD waste has potential to be used in the preparation of new commercial industrial glazes.

Corrosion experiments were performed by using different solutions (HC1, H_2SO_4 and NaOH) to evaluate their suitability under different conditions. The results show that the durability of the investigated glaze samples is higher in basic medium than in acidic medium. This trend is related to the potential interference of the divalent and relatively large calcium ion with the passageway of the mobile and liberated soluble alkali ions in the percolation pathway channels during the ion exchange process for corrosion. The chemical corrosion is markedly degraded due to high concentration HCl (0.5, 1.5 and 4.5 M), but even with these concentrations the new prepared glazes exhibit resistance for these concentrations especially C3 and C4, also the improvement of hardness is related to CKD%. Hence based on these observations, the CKD glazes are suitable to be used for glazing wall tiles which are not subjected to high pressure. In addition, these glazes can also be used for glazing table wares. The possibility of using glazes with a high CKD content (10-50 %) facilitates the use of cheap waste materials containing calcium and iron compounds and carbonates. These properties are compatible with those of commercial glazes for wall tiles and porcelain stoneware ceramics. CKD wastes, composed of an assemblage of a high level of AI_2O_3, CaO and MgO, seem to be excellent applicants and beneficial raw materials for practical purposes to improve the durability of the fabricated glaze. Generally, we need to get rid of the industrial wastes from our countries. All these positive results recommend that CKD waste seems to be useful in glaze manufacturing as a substitute for to frit glaze and then the cost will be reduced. Finally, the dissolution data, particularly with acidic and basic leaching of alkali and alkaline

earth cations, can offer greater potential for immobilization of nuclear waste.

References

1. Ismail SA, Ezz-Eldin FM (2004) Corrosion behavior of vitrified rice husk ash. Glass Technol.: Eur J Glass Sci Technol 45(5):220–226
2. Dessouki AM, Ismail SA, Ezz-Eldin FM (2005) Chemical and mechanical properties of Boro-Silicate glasses doped matrices for immobilization of medical wastes. Mat Res Innovat 9:650–662
3. da Silva RC, Pianaro SA, Tebcherani SM (2012) Preparation and characterization of glazes from combinations of different industrial wastes. Ceram Inter 38(4):2725–2731
4. El-Alaily NA, Abou-Hussein EM, Abdel-Monem YK, Abd Elaziz TD, Ezz-Eldin FM (2014) Vitrified municipal waste as a host form for high-level nuclear waste. J Radioanal Nucl Chem 299(1): 68–73
5. Francis AA, Youssef NF (2004) Glass-ceramic from industrial waste materials. Scand J Metall 33(4):236–241
6. Jasenka Z, Dragutin L, Lidija C, Marko J (2008) Estimation of chemical resistance of dental ceramics by neural network. Dent Mater 24(1):18–27
7. McMillan PW (1979) Glass-Ceramics. London, Academic Press
8. Berezhnoi AJ (1970) Glass-Ceramics And photositalls. Plenum Press, London
9. Demirkesen E, Goller G (2003) Effect of Al2O3 additions on the acid durability of a Li2O–ZnO–SiO2 glass and its glass-ceramic. Ceram Int 29(4):463–469
10. Lodding A (1992) Corrosion of Glass. In: Clark DE, Zoitos B (eds) Ceramics and Ceramic Super conductors Noyes Publications. Park Ridge, New Jersey
11. Wei D, Jin-shu C, Pei-jing T, Mi-tang W (2012) Chemical durability and weather in resistance of canasite based glass and glass-ceramics. J Non-Cryst Solids 358(21):2847–2854
12. Smith Deane K, Ron J (2003) ICDD And the the powder diffraction file past, present and future, published by alphabetical index inorganic compounds JCPDS – international centre for diffraction data, Newtown Square, A, USA
13. Casasola R, Ma RincónJ, Romero M (2012) Glass–ceramic glazes for ceramic tiles: a review. J Mater Sci 47(2):553–582
14. da Silva RC, Pianaro SA, Tebcherani SM (2012) Preparation and characterization of glazes from combinations of different industrial wastes. Ceram Int 38(4):2725–2731
15. Rocha Marcus VJ, Carvalho Hudson WP, Lacerda Livia CT, Simões G, de Souza Gerardo GB, Ramalho Teodorico C (2014) Ionic desorption in PMM–gamma-Fe_2O_3 hybrid materials induced by fast electrons: An experimental and theoretical investigation. Spectrochim Acta A 117:276–283
16. Fangfang F, Baojie C, Lifan S, Bun PEY, Hai L (2014) Multichannel transition emissions of Sm^{3+} in lithium yttrium aluminum silicate glasses and derived opalescent glass ceramics. J Alloy Compd 582:265–272
17. Ezz-Eldin FM, Nageeb WM (2001) Chemical resistance of some irradiated ceramic-glazes. Indian J Pure Ap Phy 39(8):514–524
18. Fröberg L, Kronberg T, Törnblom S, Hupaa L (2007) Chemical durability of glazed surfaces. J Eur Ceram Soc 27(2–3):1811–1816
19. Scholze H (1977) Glas. Natur, struktur und eigenschaften zweite auflage. Springer, Berlin
20. Hench L, Clark DE (1978) Physical chemistry of glass surfaces. J Non-Cryst Solids 28(1):83–105
21. Eppler R (1992). In: Clark DE, Zoitos B (eds) Corrosion of glass. Noyes Publications, New Jersey
22. Eppler R, Eppler DR (2000) Glass and glass coatings. American Ceramic Society, Westerville Ohio
23. Carlsson R (1999) Korrosion Av Glasyrer, 99-3tk, Swedish Ceramic Institute
24. Escardino A, Amoros JL, Gozalbo A, Orts MJ, Lucas F, Belda A (2002) Qualier 2002. In: Proc. of VII World Congress on Ceramic Tile Quality, Castellon, Spain, Vol. I. p. 201
25. Kronberg T, Hupa L, Fröberg L (2004) Durability of mat glazes in hydrochloric acid solution. Key Eng Mat 264–268:1565–1568
26. Vane-Tempest S, Kronberg T, Fröberg L, Hupa L (2002) Qualier 2002, in proc. of VII world congress on ceramic tile quality, castellon, Spain, Vol. I.:155
27. Fröberg L, Vane-Tempest S, Hupa L (2002) Qualier 2002. In: Proc. of VII world congress on ceramic tile quality, castellon, Spain, Vol I., p 143
28. Hupa L, Bergman R, Fröberg L, Vane-Tempest S, Hupa M, Kronberg T, Pesonen-Leinoen E, Sjoberg AM (2005) Chemical resistance and cleanability of glazed surfaces. Surf Sci 584(1):113–118
29. Bunker BC, Tallant T, Headley TJ, Turner GL, Kirkpatric RJ (1988) Structure of leached sodium borosilicate glass. Phys Chem Glasses 29(3):106–120
30. Bunker BC, Arnold GW, Beauchamp EK, Day DE (1983) Mechanisms for alkali leaching in mixed Na – K silicate glasses. J Non-Cryst Solids 58:295–322
31. Iler RK (1976) The chemistry of silica. Wiley, New York
32. Paul A (1990) Chemistry of glasses, 2nd ed. Chapman and Hall, London
33. Clark DE, Dilmore MF, Ethridge EC, Hench LL (1976) Aqueous corrosion of sodasilica and soda-lime-silica glass. J Am Ceram Soc 59(1–2):62–65
34. Budd SM, Frackiewicz J (1962) The mechanisms of chemical reaction between silicate glass and attacking agents, Part 3. Equilibrium pH of some Na_2O–CaO–SiO_2 glasses and its relationship with chemical reactivity. Phys Chem Glasses 3(4):116–120
35. Sambasiva RMV, Rajyasree Ch, Narendrudu T, Suresh S, Suneel KA, Veeraiah N, Krishna RD (2015) Physical and spectroscopic properties of multi-component Na_2O–PbO–Bi_2O_3–SiO_2 glass ceramics with Cr_2O_3 as nucleating agent. Opt Mater 47:315–322
36. Stoia M, Stefanescu M, Dippong T, Stefanescu O, Barvinschi P (2010) Low temperature synthesis of Co_2SiO_4/SiO_2 nanocomposite using a modified sol–gelmethod. J Sol Gel Technol 54(1):49–56
37. Jonynaite D, Sentvaitiene J, Beganskiene A, Kareiva A (2010) Spectroscopic analysis of blue cobalt smalt pigment. Vib Spectrosc 52(2):158–162
38. Ravneet K, Surinder S, Pandey OP (2013) Absorption spectroscopic studies on gamma irradiated bismuth borosilicate glasses. J Mol Struct 1049:386–391
39. Silviana C, Lívia LCT, Maíra dos PS, Marcus RVJ, Francisco NGE, da Silva Adilson C, Marcio PC, de Brito ADB, da Cunha EFF, Teodorico RC (2016) Synthesis, Structural Characterization, and Thermal Properties of the Poly(methylmethacrylate)/δ-FeOOH Hybrid Material: An Experimental and Theoretical Study Journal of Nanomaterials, 2016:1–7
40. Kansal I, Goel A, Tulyaganov DU, Ferreira JMF (2009) Effect of some rare-earth oxides on structure, devitrification and properties of diopside based glasses. Ceram Int 35(8):3221–3227

41. Chen A, James PF (1988) Amorphous phase separation and crystallization in a lithium silicate glass prepared by sol-gel method. J Non-Cryst Solids 100(1–3):353–358
42. El-Batal FH, Khalil EM, Hamdy YM, Zidan HM, Aziz MS, Abdelghany AM (2010) FTIR Spectral Analysis of Corrosion Mechanisms in Soda Lime Silica Glasses Doped with Transition Metal Oxides. Silicon 2:41–47
43. Cailleteau C, Weigel C, Ledieu A, Barboux P, Devreux F (2008) On the effect of glass composition in the dissolution of glasses by water. J Non Cryst Solids 354(2–9):117–123
44. La Russa MF, Ruffolo SA, Barone G, Crisci GM, Mazzoleni P, Pezzino A (2009) The use of FTIR and micro-FTIR spectroscopy: an example of application to cultural heritage, Intern. J. Spectrosc., Article ID 893528, 2009, p 5
45. Wu HF, Lin CC, Shen P (1997) Structure and dissolution of CaO-ZrO2 -TiO2 -Al2O3 - B2O3 -SiO2 glass (II). J Non-Cryst Solids 209:76–86
46. Casey WH, Bunker BC (1990). In: Hochella MF, White AF, Geochemistry Mineral-WaterInterface (eds) Mineralogical society of America, Washington, D.C, 397
47. Ulrich DR (1988) Prospects of sol-gel processes. J Non-Cryst Solids 100:174–182
48. Scherer GW (1988) Aging and drying of gels. J Non-Cryst Solids 100(1–3):77–92
49. Ezz-Eldin FM, Abd-Elaziz TD, Elalaily NA (2010) Effect of dilute HF solutions on chemical, optical, and mechanical properties of soda–lime–silica glass. J Mat Sci 45:5937–5949
50. Ezz-Eldin FM (2001) Leaching and mechanical properties of cabal glasses developed as matrices for immobilization high level wastes. Nucl Instr Meth B 183(3–4):285–300